Acta Crystallographica Section A
Foundations of Crystallography
ISSN 0108-7673

On the transition from the wurtzite to the NaCl type

H. Sowa

Institut für Angewandte Geowissenschaften I, Allgemeine und Angewandte Mineralogie, Technische Universität BH 1, Ernst-Reuter-Platz 1, D-10587 Berlin, Germany.
Correspondence e-mail: heidrun.sowa@t-online.de

Received 17 September 2000
Accepted 23 October 2000

A crystallographic interpretation of a possible transition mechanism from the wurtzite to the NaCl type is given. For this purpose, different atoms in the structures of both types are replaced by like ones, resulting in lonsdaleite-type configurations and in cubic primitive lattices, respectively. The atomic arrangements of both types correspond to homogeneous sphere packings. It is shown that a lonsdaleite configuration may be deformed into a cubic primitive lattice within the Wyckoff position $Cmcm$ $8(f)$ $m..$ $0,y,z$. Such a transition is displacive since no bonds have to be broken. The corresponding phase transformation from the wurtzite to the NaCl type can be described as a deformation of a heterogeneous sphere packing. The intermediate structure would have the symmetry $Cmc2_1$.

1. Introduction

With the exception of some mercury chalcogenides, AB compounds with four-coordinated atoms crystallize at ambient conditions either in the zinc-blende or in the wurtzite type. Both structure types are very similar from an energetic point of view (*e.g.* Yeh *et al.*, 1992; Zakharov *et al.*, 1995). One of the stable high-pressure phases for such substances is the NaCl type where each atom has six nearest neighbours. In some compounds, the NaCl type is preceded by other modifications, but there are examples for direct transformations from the zinc-blende or wurtzite type to the NaCl type. In zinc-blende ZnS itself, for instance, such a phase transition was observed at approximately 15 GPa (*e.g.* Ves *et al.*, 1990). Quite recently, a possible transition path from the zinc-blende to the NaCl type was proposed (Sowa, 2000*b*). Such a transition can be described as a deformation of a heterogeneous sphere packing and implies an intermediate structure in space group $Imm2$.

Semiconductors showing pressure-induced phase transitions from wurtzite- to NaCl-type structures are, for instance, GaN (Xia *et al.*, 1993; Ueno *et al.*, 1994), InN (Ueno *et al.*, 1994), ZnO (Gerward & Olsen, 1995) and CdSe (Yu & Gielisse, 1971). Nanocrystals of the latter compound have been studied extensively and it was shown that, during the wurtzite- to NaCl-type transition, nucleation of the high-pressure phase takes place only once in each nanocrystal (*e.g.* Tolbert & Alivisatos, 1995; Chen *et al.*, 1997). While in investigations of bulk materials usually no regard is paid to the atomic motions, in studying nanocrystals with only a limited number of atoms the microscopic changes cannot be neglected. On the basis of a theoretical investigation by Burdett & McLarnan (1981), Tolbert & Alivisatos (1995) gave a graphic description of a possible transition path.

Not only the phase transformation from the zinc-blende to the NaCl type (Sowa, 2000*b*) but also that from the NaCl to the CsCl type (Sowa, 2000*a*) can be considered as a deformation of a heterogeneous sphere packing. In both instances, investigations of the symmetry relations between low- and high-pressure phases result in feasible transition models. Therefore, it is assumed that other phase transitions occurring in simple compounds can be described in a similar way. The purpose of the present paper is to give a crystallographic interpretation of a possible mechanism for the transformation from the wurtzite to the NaCl type without breaking bonds during the transition.

2. Symmetry relations between the wurtzite and the NaCl type

Wurtzite-type AB compounds crystallize in the space group $P6_3mc$. Both A and B atoms occupy Wyckoff position $2(b)$ $\frac{1}{3},\frac{2}{3},z$ with $z = 0$ and $z = \frac{3}{8}$, respectively. Such a structure may be described as a heterogeneous sphere packing with four contacts per sphere. As was performed in previous work (Sowa, 2000*a*,*b*), the different atoms in a wurtzite-type structure are replaced by like ones. The resulting structure with space group $P6_3/mmc$ belongs to the lonsdaleite (hexagonal diamond) type. It corresponds to a configuration of the hexagonal univariant lattice complex $E2z$ (*International Tables for Crystallography*, 1995, Vol. A, ch. 14) and to a homogeneous sphere packing of type $4/6/h2$ (Fischer & Koch, unpublished material, *cf.* Fischer & Koch, 1994). The atoms occupy Wyckoff position 4(*f*) $\frac{1}{3},\frac{2}{3},z$ with $z = \frac{1}{16}$. The ideal atomic arrangement is obtained if the axial ratio is $c/a = \frac{2}{3}\times 6^{1/2} \cong 1.633$. Replacing the atoms in an NaCl-type structure (space group $Fm\bar{3}m$) with like ones results in an arrangement that corresponds to the invariant cubic lattice complex *cP* and to a sphere packing of type 6/4/*c*1 (Fischer, 1973) with six contacts per sphere. The space group of such a structure is $Pm\bar{3}m$ with a lattice parameter *a* that is half as long as that of $Fm\bar{3}m$.

On condition that no bonds are broken during the transition from the wurtzite to the NaCl type, the symmetry has to be reduced until it is possible to deform the sphere packing of type 4/6/*h*2 into a sphere packing of type 6/4/*c*1 without losing sphere contacts. The space group allowing the desired deformation must be a subgroup of both $P6_3/mmc$ and $Pm\bar{3}m$. Fig. 1 shows such a symmetry reduction: *Cmcm* is a maximal translation-equivalent subgroup of $P6_3/mmc$. The ideal lonsdaleite-type arrangement occurs within Wyckoff position 8(*f*) *m*.. $0,y,z$ with $y = \frac{1}{3}$, $z = \frac{1}{16}$ and $a/b = \frac{1}{3}\times 3^{1/2} \cong 0.5774$ and $c/b = \frac{2}{3}\times 2^{1/2} \cong 0.9428$. Starting from $Pm\bar{3}m$, removal of the threefold axes results in a translation-equivalent space group $P4/mmm$. Maintaining only the mirror planes parallel to the coordinate axes, the translation-equivalent subgroup *Pmmm* of $P4/mmm$ is obtained. Further symmetry reduction yields the class-equivalent subgroup *Pmcm* (unusual setting of *Pmma*) of *Pmmm* with doubled *c* lattice parameter. Finally, the class-equivalent subgroup *Cmcm* of *Pmcm* is reached. A doubling of the *a* and *b* lattice parameters and an origin shift by a vector $(0,\frac{1}{4},0)$ relative to the basis vectors of *Cmcm* is necessary. The *cP* configuration is found in *Cmcm* at position 8(*f*) *m*.. $0,y,z$ with $y = \frac{1}{4}$, $z = 0$ and $a = b = c$.

The analogous symmetry reduction for structures of wurtzite type leads from $P6_3mc$ to $Cmc2_1$. To obtain the undistorted structure, the atoms must occupy the Wyckoff position 4(*a*) *m*.. $0,y,z$ with $y = \frac{1}{3}$, $z = 0$ and with $y = \frac{1}{3}$, $z = \frac{3}{8}$, respectively, and $a/b = \frac{1}{3}\times 3^{1/2}$ and $c/b = \frac{2}{3}\times 2^{1/2}$ must be fulfilled. The reverse relationship between an NaCl-type and a wurtzite-type structure leads from $Fm\bar{3}m$ *via* $I4/mmm$, *Fmmm* and *Cmca* to $Cmc2_1$. The ideal NaCl arrangement is obtained if the position 4(*a*) *m*.. $0,y,z$ is occupied with $y = \frac{1}{4}$, $z = 0$ and with $y = \frac{1}{4}$, $z = \frac{1}{2}$, respectively, and $a = b = c$ is fulfilled. These relations are described in detail in Fig. 2.

The structural alterations that are necessary for the transition from an ideal lonsdaleite arrangement to a *cP* configuration can be studied by examining the possible deformations

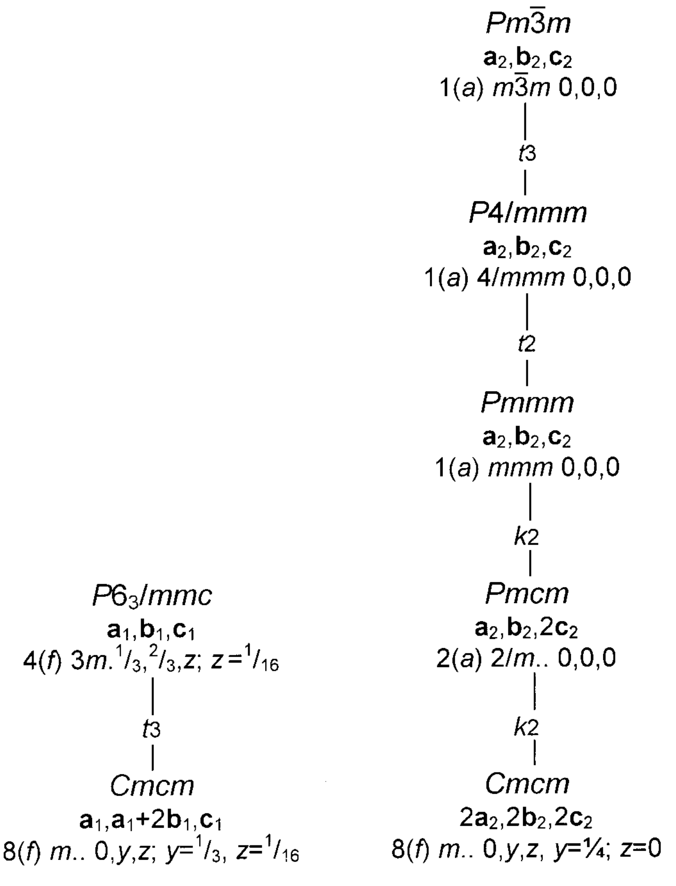

Figure 1
Symmetry relations between a lonsdaleite type and a cubic primitive lattice.

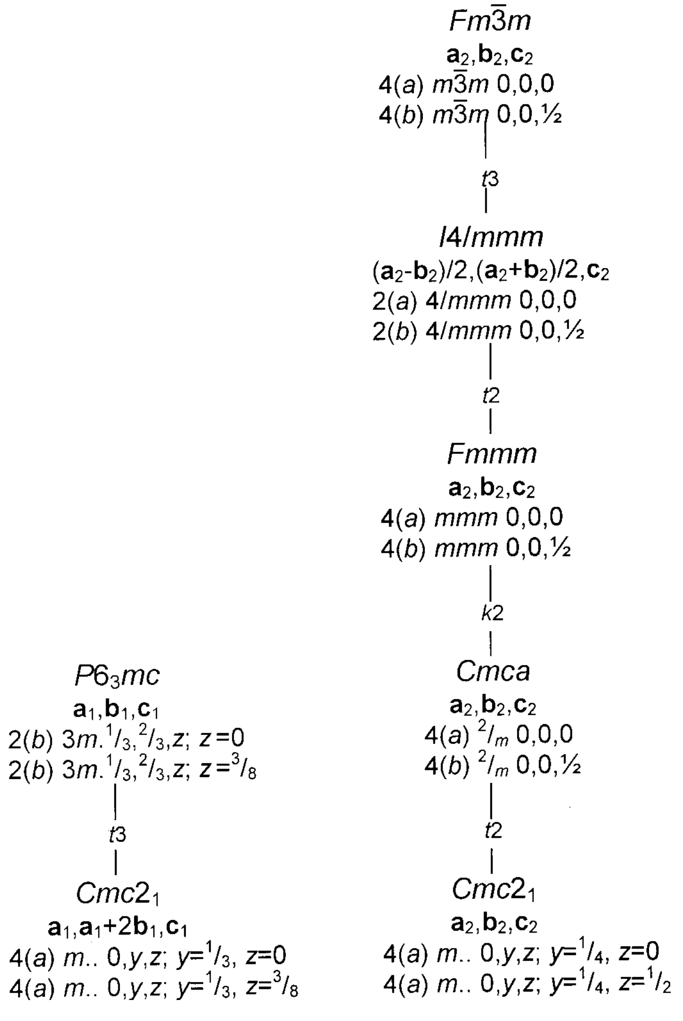

Figure 2
Symmetry relations between the structure types of wurtzite and NaCl.

Table 1
Possible neighbouring points with shortest distances to a reference point at $0,y,z$ with $0 \le y \le \frac{1}{4}$ and $0 \le z < \frac{1}{4}$ in *Cmcm* 8(*f*).

Neighbouring points	Position	Squared distances
A	$0,y,-z+\frac{1}{2}$	$d_A^2 = (4z^2-2z+\frac{1}{4})c^2$
B	$0,y,-z-\frac{1}{2}$	$d_B^2 = (4z^2+2z+\frac{1}{4})c^2$
C	$0,-y,-z$	$d_C^2 = 4y^2b^2+4z^2c^2$
D	$\frac{1}{2},-y+\frac{1}{2},-z$ $-\frac{1}{2},-y+\frac{1}{2},-z$	$d_D^2 = \frac{1}{4}a^2+(4y^2-2y+\frac{1}{4})b^2+4z^2c^2$
E	$0,-y+1,-z$	$d_E^2 = (4y^2-4y+1)b^2+4z^2c^2$
F	$\frac{1}{2},y-\frac{1}{2},z$ $\frac{1}{2},y+\frac{1}{2},z$ $-\frac{1}{2},y+\frac{1}{2},z$ $-\frac{1}{2},y-\frac{1}{2},z$	$d_F^2 = \frac{1}{4}a^2+\frac{1}{4}b^2$
G	$1,y,z$ $-1,y,z$	$d_G^2 = a^2$
H	$0,y+1,z$ $0,y-1,z$	$d_H^2 = b^2$

of sphere packings of type $4/6/h2$ within the lattice complex *.n.* C_c2yz [characteristic Wyckoff position *Cmcm* 8(*f*) *m*.. $0,y,z$; *cf. International Tables for Crystallography* (1995), Vol. A, ch. 14]. This lattice complex has four parameters that may be varied: the positional parameters y and z and the two axial ratios a/b and c/b. Since there is at present no information available about sphere configurations with the corresponding symmetry, *.n.* C_c2yz was investigated in the same way as for the lattice complexes $R6x\bar{x}z$ [$R\bar{3}m$ 18(*h*)] (Sowa & Koch, 1999), $00\frac{1}{4}$ 2_1.. C_cF1y [*Cmcm* 4(*c*)] (Sowa, 2000*a*), and $0\frac{1}{4}0$ .2. A_aB_b1z [*Imma* 4(*e*)] (Sowa, 2000*b*).

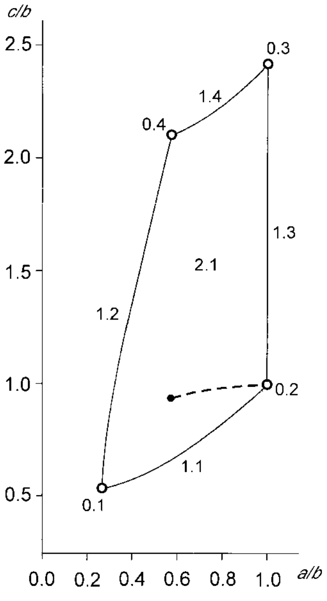

Figure 3
Projection on the a/b–c/b plane of the parameter fields of sphere-packing types bounding $4/6/h2$ in *Cmcm* 8(*f*) $0,y,z$ with $0 \le y \le \frac{1}{4}$ and $0 \le z < \frac{1}{4}$. All sphere packings are designated by the corresponding generation classes. The solid circle shows the parameters of the ideal lonsdaleite arrangement. The dashed line marks the proposed transition path.

3. Sphere packings belonging to *.n.* C_c2yz [*Cmcm* 8(*f*)]

The lattice complex *.n.* C_c2yz occurs not only in Wyckoff position *Cmcm* 8(*f*) but also in the general position of *Ama*2 (*cf. International Tables for Crystallography*, 1995, Vol. A, ch. 14; Fischer *et al.*, 1973). In addition, it can be found as a limiting complex (Koch, 1984; Koch & Fischer, 1985, and references therein) in the general positions of *Pnma*, *Pbcn*, *Pbcm*, *Pnna* and $C222_1$ (Engel *et al.*, 1984). Therefore, all sphere configurations that occur in Wyckoff position *Cmcm* 8(*f*) can be found with site symmetry 1 in these space groups.

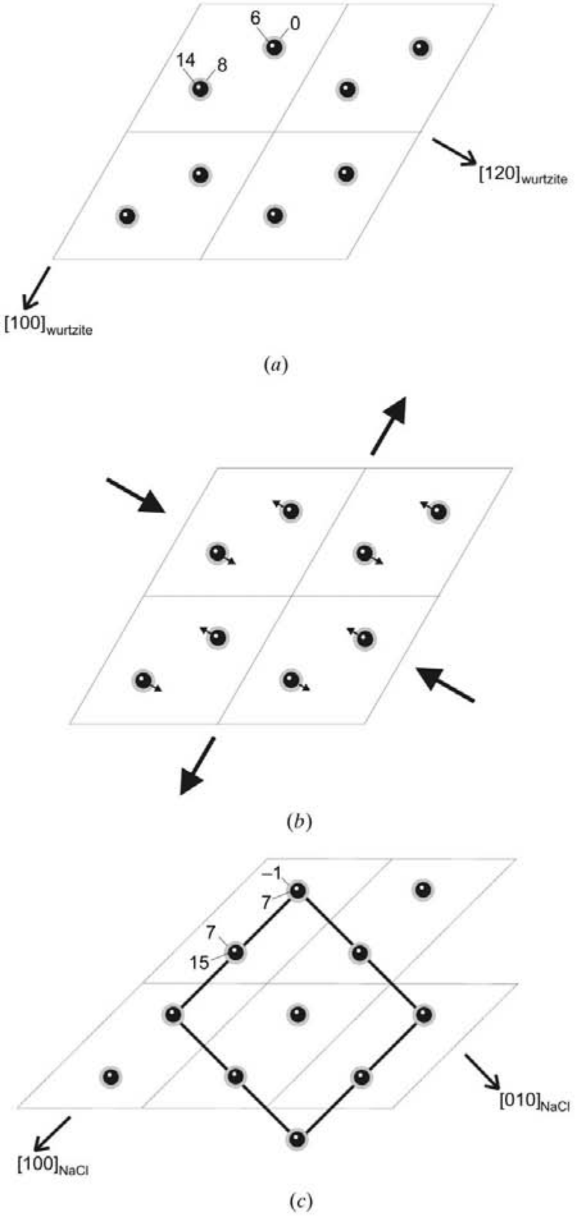

Figure 4
Schematic representation of the proposed mechanism of the wurtzite- to NaCl-type transition. The z coordinates of the atoms are given in $n/16$. (*a*) Atomic arrangement of a wurtzite-type structure. (*b*) Necessary structural changes: small arrows indicate the atomic movements, bold arrows the metrical changes. (*c*) NaCl-type structure after the phase transition. Thin lines show the wurtzite-type unit cell, heavy lines that of the NaCl type [the origin has to be shifted by $(0,0,\frac{1}{16})$].

Table 2
Sphere-packing conditions for *.n.* C_c2yz [*Cmcm* 8(*f*)].

Sphere-packing type	Generation class	Neighbouring points	Sphere-packing conditions				
4/6/*h*2	2.1	*ACD*	$4y^2b^2+(2z-\frac{1}{4})c^2 = 0$; $a^2-(8y-1)b^2 = 0$				
6/4/*c*1	2.2	*ACF*	$4y^2b^2+(2z-\frac{1}{4})c^2 = 0$; $\frac{1}{4}a^2-(4y^2-\frac{1}{4})b^2-4z^2c^2 = 0$				
7/4/*o*1	2.3	*ADF*	$\frac{1}{4}a^2+(4y^2-2y+\frac{1}{4})b^2+(2z-\frac{1}{4})c^2 = 0$; $(4y^2-2y)b^2+4z^2c^2 = 0$				
5/4/*h*5	1.1	*ABCD*	2.1; $z = 0$				
6/3/*o*2	1.2	*ACDG*	2.1; $a^2-4y^2b^2-4z^2c^2 = 0$				
5/4/*t*6	1.3	*ACDE*	2.1; $y = \frac{1}{4}$; $a = b$				
8/3/*o*2	1.4	*ACDF*	2.1; 2.3				
7/4/*o*1	1.5	*ACEF*	2.2; $y = \frac{1}{4}$				
8/3/*h*4	1.6	*ACFG*	2.2; $a = \frac{1}{3}\times 3^{1/2}b$				
9/3/*o*1	1.7	*ADFG*	2.3; $a = \frac{1}{3}\times 3^{1/2}b$				
8/3/*h*4	1.8	*ACFH*	2.2; $a = 3^{1/2}b$				
7/3/*o*1	0.1	*ABCDG*	$y = 1-\frac{1}{2}\times 3^{1/2}$;	$z = 0$;	$a/b = 2-3^{1/2}$;	$c/b = 2(2-3^{1/2})$;	$\rho = 56.1\%$
6/4/*c*1	0.2	*ABCDE*	$y = \frac{1}{4}$;	$z = 0$;	$a/b = 1$;	$c/b = 1$;	$\rho = 52.4\%$
9/3/*t*2	0.3	*ACDEF*	$y = \frac{1}{4}$;	$z = \frac{1}{4}(2^{1/2}-1)$;	$a/b = 1$;	$c/b = 2^{1/2}+1$;	$\rho = 60.5\%$
10/3/*h*2	0.4	*ACDFG*	$y = \frac{1}{16}$;	$z^2 = \frac{1}{8}(5-2\times 6^{1/2})$;	$a/b = \frac{1}{3}\times 3^{1/2}$;	$c/b = \frac{2}{3}(2^{1/2}+3^{1/2})$;	$\rho = 66.6\%$
9/3/*o*1	0.5	*ACEFH*	$y = \frac{1}{4}$;	$z = \frac{1}{2}\times 3^{1/2}-\frac{3}{4}$;	$a/b = 3^{1/2}$;	$c/b = 2+3^{1/2}$;	$\rho = 64.8\%$

As pointed out by Fischer (1991), for geometrical investigations of a certain Wyckoff position of a space group G, it is sufficient to regard only one asymmetric unit of the Euclidean normalizer $N_E(G)$ (*cf.* Fischer & Koch, 1983). The Euclidean normalizer N_E (*Cmcm*) is *Pmmm* with $\mathbf{a}' = \frac{1}{2}\mathbf{a}$, $\mathbf{b}' = \frac{1}{2}\mathbf{b}$, $\mathbf{c}' = \frac{1}{2}\mathbf{c}$ (*cf. International Tables for Crystallography*, 1995, Vol. A, ch. 15), *i.e.* a supergroup of index 4 of *Cmcm*. For the following investigations of Wyckoff position 8(*f*) $0,y,z$ of *Cmcm*, the range $0 \le y \le \frac{1}{4}$, $0 \le z < \frac{1}{4}$ was chosen.

As described in previous publications (Sowa & Koch, 1999; Sowa, 2000*a*,*b*), all symmetrically equivalent points with shortest distances were determined for any reference point being situated at $0,y,z$ in the asymmetric unit considered. There are 14 such possible neighbouring points. Some of them form pairs or quadrilaterals with equal distances to the reference point. Hence, only eight different kinds of possible neighbours have to be distinguished, which are designated by the capital letters A to H. Table 1 shows the position of each neighbour referred to the reference point at $0,y,z$ and its squared distance to this point. In the investigation of the parameter range $0 \le y \le \frac{1}{4}$, $0 \le z < \frac{1}{4}$, all sphere configurations were derived. In total, there are 61 different possibilities for generating sphere configurations within the investigated parameter region. 16 of these correspond to homogeneous sphere packings belonging to 12 different types. Owing to the large number of sphere configurations with point-group, rod-group or layer-group symmetry, only sphere packings are listed in Table 2: They are symbolized according to Fischer (1973, 1991). Each sphere-packing type is characterized by a symbol $k/m/fn$: k is the number of contacts per sphere, m gives the size of the shortest mesh, f indicates the highest crystal family for sphere packings of that type and n is an arbitrary number. The second column displays the corresponding generation class (Fischer, 1991) designated by a symbol $g.h$, where g gives its number of degrees of freedom and h is an arbitrary number. The third column of Table 2 lists the nearest neighbours of the reference point. In the fourth column, the sphere-packing conditions are given that must be fulfilled by the positional parameters of the sphere centres and by the metrical parameters of the unit cell. Three generation classes of sphere packings show two degrees of freedom and eight classes have one degree of freedom. For the five classes with no degree of freedom, the y and z coordinates of the centre of the reference sphere, the a/b and c/b axial ratios, and the space filling ρ are listed. With the exception of types 6/3/*o*2 (1.2) and 8/3/*o*2 (1.4), sphere packings of all types may also be generated with higher symmetry, because lattice complex *.n.* C_c2yz [*Cmcm* 8(*f*)] comprises certain lattice complexes as limiting forms. For each sphere-packing type occurring in *Cmcm* 8(*f*), Table 3 shows the highest supergroup of *Cmcm* that allows sphere packings of that type. In addition, metrical and positional parameters are given that refer to the lowest density of that type (column 2). The corresponding parameters in *Cmcm* 8(*f*) are tabulated in column 3.

4. The lonsdaleite- to *cP*-type transition

An ideal lonsdaleite configuration corresponds to a sphere packing of type 4/6/*h*2 with minimal density ($\rho = 34.0\%$). In *Cmcm* 8(*f*), this type occurs with two degrees of freedom and refers to the generation class 2.1. The corresponding sphere-packing conditions are

$$4y^2b^2 + 2zc^2 - \tfrac{1}{4}c^2 = 0 \quad \text{and} \quad a^2 - 8yb^2 + b^2 = 0. \qquad (1)$$

The two-dimensional parameter region of 4/6/*h*2 (2.1) is bounded by the one-dimensional regions of the generation classes 1.1, 1.2, 1.3 and 1.4, and by the points referring to the classes 0.1, 0.2, 0.3 and 0.4. Fig. 3 shows a projection on the a/b–c/b plane of the parameter regions of these sphere packing types with $0 \le y \le \frac{1}{4}$, $0 \le z < \frac{1}{4}$. The ideal lonsdaleite type occurs at $y = \frac{1}{16}$, $z = \frac{1}{16}$ with $a/b = \frac{1}{3}\times 3^{1/2}$ and $c/b = \frac{2}{3}\times 2^{1/2}$. In principle, a sphere packing of type 4/6/*h*2 may be deformed

Table 3
Highest possible symmetry of sphere packings occurring in *Cmcm* 8(*f*).

Sphere-packing type	Highest possible symmetry and parameters at minimal density	Corresponding parameters in *Cmcm* 8(*f*)
6/4/*c*1	$Pm\bar{3}m$ 1(*a*) 0,0,0	$y=\frac{1}{4}$; $z=0$; $a/b=1$; $c/b=1$ $y=0$; $z=\frac{1}{8}$; $a/b=1$; $c/b=2\times2^{1/2}$
8/3/*h*4	$P6/mmm$ 1(*a*) 0,0,0 $c/a=1$	$y=0$; $z=\frac{1}{8}$; $a/b=\frac{1}{3}\times3^{1/2}$; $c/b=\frac{4}{3}\times3^{1/2}$ $y=0$; $z=\frac{1}{8}$; $a/b=3^{1/2}$; $c/b=4$
5/4/*h*5	$P6/mmm$ 2(*c*) $\frac{1}{3},\frac{2}{3},0$ $c/a=\frac{1}{3}\times3^{1/2}$	$y=\frac{1}{16}$; $z=0$; $a/b=\frac{1}{3}\times3^{1/2}$; $c/b=\frac{2}{3}$
4/6/*h*2	$P6_3/mmc$ 4(*f*) $\frac{1}{3},\frac{2}{3},z$; $z=\frac{1}{16}$ $c/a=\frac{2}{3}6^{1/2}$	$y=\frac{1}{16}$; $z=\frac{1}{16}$; $a/b=\frac{1}{3}\times3^{1/2}$; $c/b=\frac{2}{3}\times2^{1/2}$
10/3/*h*2	$P6_3/mmc$ 4(*f*) $\frac{1}{3},\frac{2}{3},z$; $z=[\frac{1}{8}(5-2\times6^{1/2})]^{1/2}$ $c/a=\frac{2}{3}6^{1/2}+2$	$y=\frac{1}{16}$; $z=[\frac{1}{8}(5-2\times6^{1/2})]^{1/2}$; $a/b=\frac{1}{3}\times3^{1/2}$; $c/b=\frac{2}{3}(2^{1/2}+3^{1/2})$
5/4/*t*6	$I4/mmm$ 4(*e*) $0,0,z$; $z=\frac{3}{16}$ $c/a=2$	$y=\frac{1}{4}$; $z=\frac{1}{16}$; $a/b=1$; $c/b=2^{1/2}$
9/3/*t*2	$I4/mmm$ 4(*e*) $0,0,z$; $z=\frac{1}{2}-\frac{1}{2}\times2^{1/2}$ $c/a=2^{1/2}+2$	$y=\frac{1}{4}$; $z=\frac{1}{4}(2^{1/2}-1)$; $a/b=1$; $c/b=2^{1/2}+1$
7/4/*o*1	$Fmmm$ 8(*i*) $0,0,z$; $z=0.1414$ $a/b=1.1976$; $c/b=2.7578$	$y=\frac{1}{4}$; $z=0.1086$; $a/b=1.1976$; $c/b=2.7578$ $y=\frac{1}{4}$; $z=0.1086$; $a/b=0.8350$; $c/b=2.3028$
9/3/*o*1	$Fmmm$ 8(*i*) $0,0,z$; $z=1-\frac{1}{2}\times3^{1/2}$ $a/b=3^{1/2}$; $c/b=3^{1/2}+2$	$y=\frac{1}{4}$; $z=\frac{1}{2}\times3^{1/2}-\frac{3}{4}$; $a/b=3^{1/2}$; $c/b=3^{1/2}+2$ $y=\frac{1}{4}$; $z=\frac{1}{2}\times3^{1/2}-\frac{3}{4}$; $a/b=\frac{1}{3}\times3^{1/2}$; $c/b=\frac{2}{3}\times3^{1/2}+1$
7/3/*o*1	$Cmmm$ 4(*i*) $0,y,0$; $y=1-\frac{1}{2}\times3^{1/2}$ $a/b=2-3^{1/2}$; $c/b=2-3^{1/2}$	$y=1-\frac{1}{2}\times3^{1/2}$; $z=0$; $a/b=2-3^{1/2}$; $c/b=2(2-3^{1/2})$
6/3/*o*2	$Cmcm$ 8(*f*) $0,y,z$	$y=0.1368$; $z=0.0779$; $a/b=0.3068$; $c/b=0.8915$
8/3/*o*2	$Cmcm$ 8(*f*) $0,y,z$	$y=0.2188$; $z=0.1071$; $a/b=\frac{1}{2}\times3^{1/2}$; $c/b=2.3150$

without breaking of bonds into sphere packings of all the types mentioned above. All of them show higher densities ρ and higher contact numbers compared with 4/6/*h*2. However, in the case of wurtzite-type crystal structures with two kinds of atom, neighbours labelled *F*, *G*, *H* denote like atoms and *A*, *B*, *C*, *D* and *E* represent unlike atoms compared with the reference atom. As *A*, *C* and *D* are the neighbours in a sphere packing of type 4/6/*h*2, the only possible additional neighbours in a partly ionic compound are *B* and *E*, giving rise to 5/4/*h*5 (1.1) and 5/4/*t*6 (1.3) with one degree of freedom, or 6/4/*c*1 (0.2) with no degree of freedom. In sphere packings of types 5/4/*h*5 and 5/4/*t*6, each sphere has five nearest neighbours forming a coordination polyhedron with trigonal bipyramidal or tetragonal pyramidal shape, respectively. However, the actual high-pressure phases for wurtzite-type compounds belong to the NaCl type. The appropriate homogeneous sphere-packing type is 6/4/*c*1 and the undistorted *cP* configuration is found at $y=\frac{1}{4}$, $z=0$ and $a=b=c$ (*cf*. Fig. 1 and Table 3). In addition, even if only like atoms are considered, all other sphere-packing types that are given in Table 3 but not occurring in Fig. 3 cannot be reached without breaking bonds when starting from 4/6/*h*2.

Fig. 4 shows the corresponding structural changes that are necessary for transforming the wurtzite into the NaCl type. During the transition, all atoms are shifted in a cooperative manner within the $(\bar{2}10)$ planes of the wurtzite-type structure by $\frac{1}{16}\times3^{1/2}\mathbf{a}+\frac{1}{16}\mathbf{c}$. Simultaneously, the unit cell has to be contracted along the [120] and [001] directions while it must be elongated parallel to [100].

Such a phase transition yields the following orientation relations: $[001]_{\rm wurtzite}$ is parallel to $[001]_{\rm NaCl}$, $[100]_{\rm wurtzite}$ corresponds to $[100]_{\rm NaCl}$ and $[120]_{\rm wurtzite}$ to $[010]_{\rm NaCl}$.

As has been noted in previous papers (Sowa, 2000*a*,*b*), the true transition path cannot be determined geometrically. However, similar to the structural transition from the diamond type to a cubic primitive lattice (corresponding to a transition from the zinc-blende to the NaCl type), a model can be constructed implying that ten of the twelve next-nearest neighbours in a lonsdaleite structure keep equal distances to the reference atom. Then, in addition to the sphere-packing conditions, the following equation has to be fulfilled:

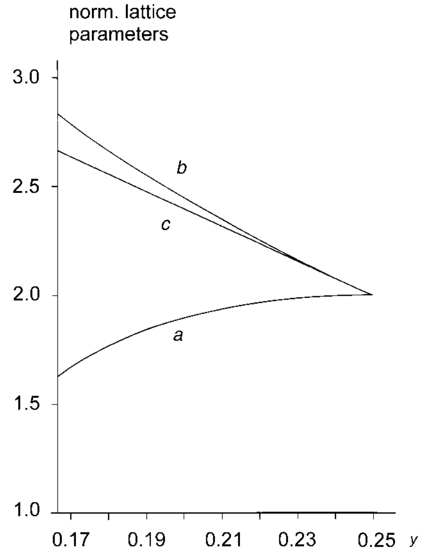

Figure 5
Variations of the normalized lattice parameters (shortest interatomic distance $d=1$) depending on the positional parameter *y* during the transformation from the wurtzite to the NaCl type (transition model with ten equal distances to the next-nearest neighbours during the transition).

$$a^2 + b^2(1 - 16y^2) - c^2 = 0. \qquad (2)$$

The location of an undistorted lonsdaleite type and the path corresponding to (2) are marked in Fig. 3.

Fig. 5 shows the variations of the unit-cell parameters' dependence on y for such a model with four nearest neighbours at a distance of $d = 1$ from the reference atom. Fig. 6 displays the corresponding normalized interatomic distances.

The mechanism of the transition from the wurtzite to the NaCl type described above agrees with that proposed by Tolbert & Alivisatos (1995). These authors, however, give a rather descriptive model of the necessary atomic motions, whereas in the present paper a possibility is offered to analyse such a mechanism on the basis of crystallographic considerations. Though real crystal structures may not show such an ideal behaviour, the given geometric relations should facilitate energetic calculations concerning the phase transition.

While there is experimental evidence for the wurtzite- to NaCl-type transition at elevated pressures, the analogous transformation in elements is unknown since no high-pressure investigations of materials with lonsdaleite-type structures seem to exist yet.

5. The reverse transition

When pressure is released, the NaCl-type phase of CdSe not only undergoes a transition to a modification with a wurtzite-type crystal structure but, in addition, CdSe with the zinc-blende type occurs (*e.g.* Tolbert & Alivisatos, 1995). Considering the bonds that have to be broken in the NaCl type, such a behaviour can easily be understood. During the transformation leading to the zinc-blende or the wurtzite type, two of the six bonds per atom are lost. In Figs. 7(*a*) and (*b*), one unit cell of an NaCl-type structure is shown. Provided that the proposed transition mechanisms occur, the pattern of broken bonds (dashed lines) in two sets of the {100} planes, namely (010) and (001), is the same for the transition to the zinc-blende (Fig. 7*a*) and to the wurtzite type (Fig. 7*b*). The only difference can be seen in the third set of such planes: In (100), the broken bonds form zigzag chains if the transition leads to the zinc-blende type while meandering chains are found if the wurtzite type is obtained. Figs. 7(*a*) and (*b*) display also the different site symmetries $mm2$ and m of the atoms in the intermediate structures, respectively. In both cases, all atoms move slightly within these planes (Figs. 7*c*, *d*) and the NaCl-type unit cell is contracted perpendicular to these planes. During the transition from the NaCl to the zinc-blende type, the unit cell is elongated parallel to [011] and [01$\bar{1}$], but by a different factor (Fig. 7*e*) and, simultaneously, the atoms are shifted by $\frac{1}{16}$ of the longer face diagonal. During the NaCl- to wurtzite-type transformation, the atoms move along $\langle 034 \rangle$ directions and the unit cell is elongated parallel to [010] and [001] (Fig. 7*f*). It is assumed that the energy barrier is very similar for both transitions.

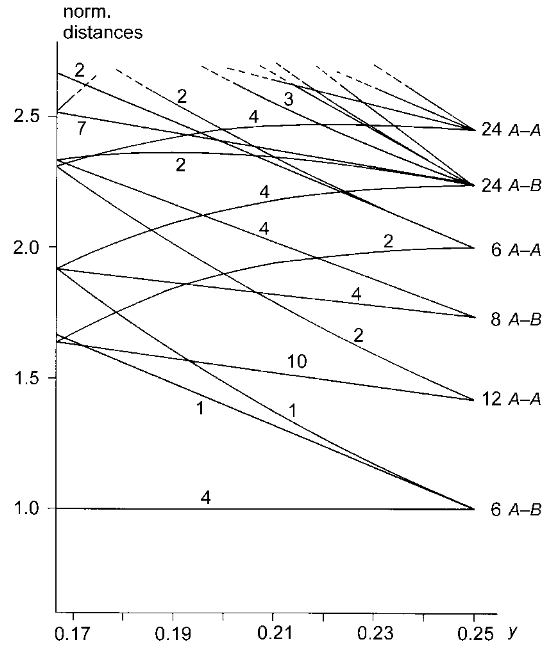

Figure 6
Variations of the normalized interatomic distances (shortest interatomic distance $d = 1$) depending on the positional parameter y during the transformation from the wurtzite to the NaCl type (transition model with ten next-nearest neighbours with equal distances). The numbers of equal distances are given.

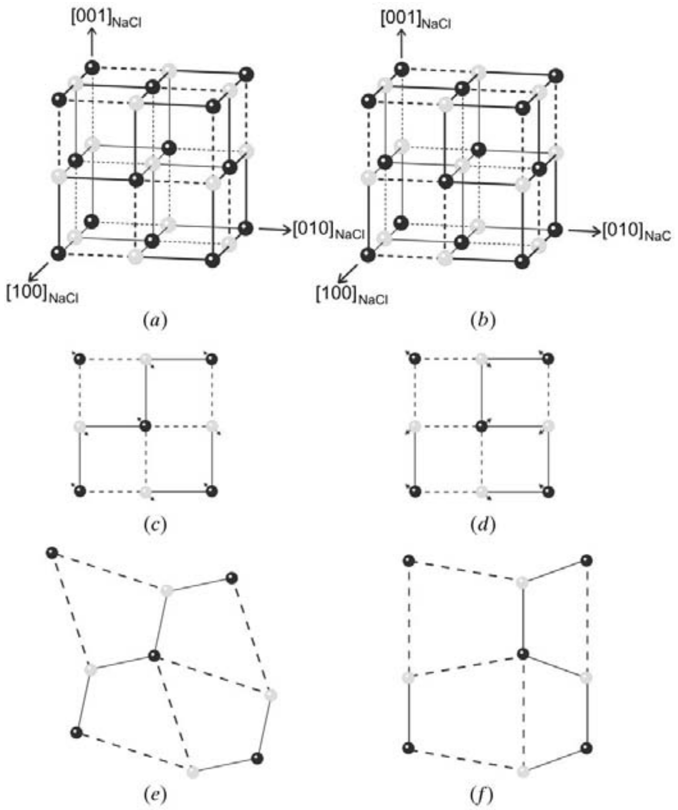

Figure 7
Pattern of breaking bonds for the phase transition from the NaCl to (*a*) the zinc-blende and (*b*) the wurtzite type. Atomic movements within one plane during the transition to (*c*) the zinc-blende and (*d*) the wurtzite type. Resulting atomic arrangements after necessary metrical variations during the transition to (*e*) the zinc-blende and (*f*) the wurtzite type.

I would like to thank Professor Dr E. Koch, Marburg, for many helpful discussions.

References

Burdett, J. K. & McLarnan, T. J. (1981). *J. Chem. Phys.* **75**, 5764–5773.

Chen, C. C., Herhold, A. B., Johnson, C. S. & Alivisatos, A. P. (1997). *Science*, **276**, 398–401.

Engel, P., Matsumoto, T., Steinmann, G. & Wondratschek, H. (1984). *Z. Kristallogr.* Suppl. Issue 1.

Fischer, W. (1973). *Z. Kristallogr.* **138**, 129–146.

Fischer, W. (1991). *Z. Kristallogr.* **194**, 67–85.

Fischer, W., Burzlaff, H., Hellner, E. & Donnay, J. D. H. (1973). *Space Groups and Lattice Complexes. US Natl Bur. Stand. Monograph*, No. 134. Washington: National Bureau of Standards.

Fischer, W. & Koch, E. (1983). *Acta Cryst.* A**39**, 907–915.

Fischer, W. & Koch, E. (1994). *Z. Kristallogr.* Suppl. Issue 8, 208.

Gerward, L. & Olsen, J. St. (1995). *J. Synchrotron Rad.* **2**, 233–235.

International Tables for Crystallography (1995). Vol. A, edited by Th. Hahn. Dordrecht: Kluwer Academic Publishers.

Koch, E. (1984). *Z. Kristallogr.* **166**, 23–52.

Koch, E. & Fischer, W. (1985). *Acta Cryst.* A**41**, 421–426.

Sowa, H. (2000*a*). *Acta Cryst.* A**56**, 288–299.

Sowa, H. (2000*b*). *Z. Kristallogr.* **215**, 335–342.

Sowa, H. & Koch, E. (1999). *Z. Kristallogr.* **214**, 316–323.

Tolbert, S. H. & Alivisatos, A. P. (1995). *J. Chem. Phys.* **102**, 4642–4656.

Ueno, M., Yoshida, M., Onodera, A., Shimomura, O. & Takemura, A. (1994). *Phys. Rev. B*, **49**, 14–21.

Ves, S., Schwarz, U., Christensen, N. E., Syassen, K. & Cardona, M. (1990). *Phys. Rev. B*, **42**, 9113–9118.

Xia, H., Xia, Q. & Ruoff, A. L. (1993). *Phys. Rev. B*, **47**, 12925–12928.

Yeh, C. Y., Lu, Z. W., Froyen, S. & Zunger, A. (1992). *Phys. Rev. B*, 46, 10086–10097.

Yu, W. C. & Gielisse, P. J. (1971). *Mater. Res. Bull.* **6**, 621–638.

Zakharov, O., Rubio, A. & Cohen, M. (1995). *Phys. Rev. B*, **51**, 4926–4930.